Conceptual design and sizing optimization based on minimum energy consumption of lift-cruise type eVTOL aircraft powered by battery and fuel cell for urban air mobility

Conceptual design and sizing optimization based on minimum energy consumption of lift-cruise type eVTOL aircraft powered by battery and fuel cell for urban air mobility

Teresa Donateo[1], Hasan Çınar[2],

[1] Department of Engineering for Innovation, University of Salento, Lecce, 73100, Italy
[2] Faculty of Aeronautics and Astronautics, Iskenderun Technical University, Iskenderun, 31200, Turkey

teresa.donateo@unisalento.it

Abstract. In conceptual studies and prototypes of aerial vehicles for Urban Air Mobility, batteries are generally adopted as only energy sources. However, batteries have a long charging time that is not suitable for consecutive flights, and a low energy density that limits the range and flight time of the aircraft. For this reason, the hybrid propulsion solution consisting of a battery and a fuel cell has attracted attention in aviation in recent years. This study proposes the conceptual design of a VTOL (Vertical Take-Off and Landing) aircraft for passenger transportation in metropolitan areas by the synergic optimization of the aircraft configuration and the sizing of the propulsion system aimed at minimizing the power request in cruise. In the proposed conceptual design method, VTOL type aircraft is powered by either the battery or the fuel cell according to the flight phase. A multivariate nonlinear optimization problem using as goal the minimization of the fuel cell size is solved. The optimal values of battery size, wing loading, aspect ratio, endurance speed, aircraft weight, maximum lift coefficient, disk loading, rotor solidity, and zero-lift drag coefficient are determined from the solution of the optimization problem.

1. Introduction

Urban air mobility (UAM) includes cases such as passenger transport within metropolises and between neighbouring cities, emergency transport, and cargo delivery [1]. The concept of UAM is not new (its first examples date back to the 1950s [2]) but continued only as a helicopter service until recently when its applicability to UAM has increased due to the growing concerns on traffic congestion, noise, and harmful emissions. Companies such as Uber Elevate, Hyundai, eHANG, Boeing-Aurora Transmative, Grab and BLADE carry out research and development activities on economic feasibility, safety, and critical design issue in UAM passengers transportation in metropolises [3]. In fact, for UAM to become widespread, it needs still improvement in terms of operation and maintenance cost sustainability, public trust and acceptance, infrastructure suitability, and aircraft range [4].

The VTOL-type aircraft (VTOL (Vertical Take-Off and Landing)) are more suitable for passenger transportation in urban air mobility because they provide vertical take-off and landing. There are four types of VTOL aircraft in general: lift-cruise, rotary-wing, tilt-rotor, and tilt-wing [5]. Among these, rotary-wing aircraft are superior in terms of hover and manoeuvrability [6]. In addition, they have a more compact structure compared to other VTOL aircraft types. However, due to their higher power consumption, they are generally more suitable for short-distance passenger transportation[6]. Since lift-

cruising, tilt-wing, and tilt-rotor type aircraft have a fixed-wing, their lift forces are higher than rotary-wing VTOL aircraft [3]. The tilt-rotor and tilt-wing aircraft require special equipment as they change their mode during flight. In lift-cruise type aircraft, vertical and horizontal movements are provided by different propellers. Therefore, additional drag occurs in lift-cruise aircraft. In this study, sizing optimization studies of the hybrid propulsion system consisting of fuel cell and battery are carried out for a lift-cruise VTOL aircraft.

Electric power systems are more suitable for VTOL-type aircraft used for passenger transportation in Urban air mobility, rather than piston or turbine engines [6]. There are many reasons for this, such as the aircraft being VTOL type, fossil fuel dependency, harmful emissions, and noise. However, in today's technology, batteries are not enough dense for long-range flights. In addition, the charging times of the batteries are long and imposes restrictions for consecutive flights. According to the report published by Uber [7], it is expected that the time of the charge between flights in electric VTOL (eVTOL) should be less than 7 minutes. To ensure this condition, the batteries are charged fast between flights, and on the contrary, they are charged slowly at night. However, this practice causes serious reductions in the life of the batteries [8] . In this context, hybridization can be suggested to solve these problems related to low energy density and the long charging time of batteries. In a previous investigation of one of the authors, [9] hybridization with internal combustion engines is considered. In this study, hydrogen is considered as a secondary energy source and a fuel cell is used to power the electric motors together with the batteries.

Battery and fuel cell systems have different characteristics in terms of energy/power density, dynamic response speed, service life, and energy weight ratio. The energy density refers to the energy stored per unit mass or volume and is directly related to the maximum endurance that can be obtained. Power density refers to the power that can be drawn from the energy source per unit mass. In the case of the fuel cell system, the available energy is associated mainly to the specification of the hydrogen tank. Pressurized hydrogen at 350-700 bar is usually considered for land and air transportation [10]. The power of the system, on the contrary, depends on the size of the fuel cell in terms of nominal voltage and active area.

The comparison of energy components in terms of gravimetric energy density, volumetric energy density, total efficiency, and lifetime is given in Figure 1 In this figure, adapted from the literature [11]-[13]., ``fuel cell'' is meant as the whole system including the converter (fuel cell) and its power source (hydrogen stored in a pressurized vessel).

Even among batteries of the same family (like for example lithium-ion batteries), it is possible to define a trade-off between power density and energy density according to their design and manufacturing (see Table 1). In the case of batteries, energy and power are linked so it is necessary to keep in mind the relation between them [9]. In general, batteries have a higher power density than fuel cells [10].

The main contribution of this study is to present a sizing optimization procedure based on minimum energy consumption for a lift cruise eVTOL-type hybrid aircraft. This sizing optimization is based on the minimization of power consumption of the aircraft and includes both the aircraft configuration and the propulsive system. The flight profile of the aircraft consists of hover, transition+climb, acceleration+climb, cruising, deceleration+descent, transition+descent, and hover+descent flight modes. Among these flight modes, hover and transition+climb modes are the more critical in terms of power request while the cruise mode (horizontal flight modes) is the critical phase in terms of energy request because it directly affects the endurance. To better exploit the specification of the battery and the fuel cell system, in this investigation, battery provides energy in the hover and transition+climb flight modes of the aircraft, while the fuel cell is used for the cruising and accel+climb flight modes of the aircraft. This approach has been accepted in the literature and has examples for some UAVs (example of [14]-[16]). Nevertheless, after this preliminary work, more advanced energy management strategies will be taken into account [17] .

Electric vehicles with batteries and/or hydrogen systems are considered as zero-emissions vehicles because they do not generate greenhouse and harmful gases during the operation. However, both electricity and hydrogen are energy carriers that can be obtained with different processes from the primary energy sources and therefore, can have a not negligible indirect environmental impact [18][19].

This aspect is shortly addressed in the last section of this paper but a detailed comparison with the previous results on hybrid, conventionally and battery-powered vehicles for UAM [9] in terms of endurance and direct and indirect emissions of CO2 will be performed as further investigation. To this scope, the take-off weight of the aircraft was chosen equal to 1800 kg in the present investigation.

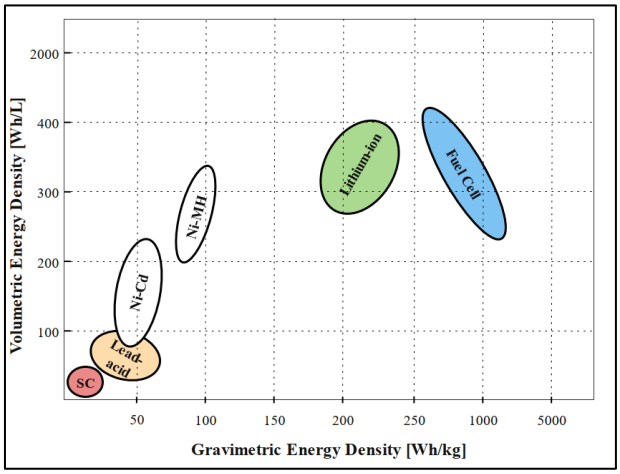

Figure 1. Comparison of energy components **[11]-[13].**

Table 1. Power and energy density of battery and fuel cell [10][20].

Energy Source	Power Density (W/kg)	Energy Density (Wh/kg)
PEM Fuel Cell system	300-2000	600-1000
Battery	500-2800	40-350

2. Methodology

In this study, the report published by Uber[7] is taken as a reference for the flight profile and mission requirements of the lift-cruising type aircraft that will serve for urban air mobility. The design of this aircraft is made to carry 3 or 4 passengers in 60 miles (96 km) range.

2.1. Mission profile and performance requirement of the lift-cruising aircraft

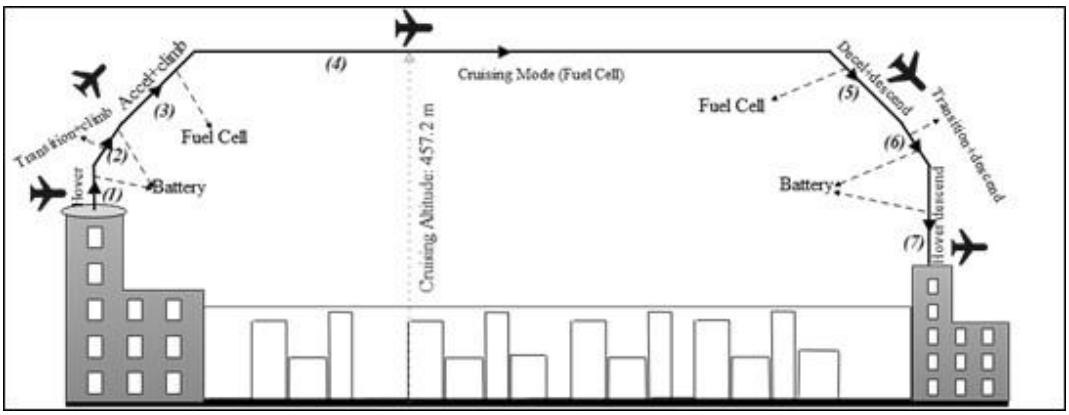

Figure 2. The flight profile of the lift-cruise VTOL aircraft.

A representation of the flight profile of the aircraft is given in Figure 2 while the mission requirements for each flight mode of the aircraft (hover, transition+climb, accel+climb, cruise, descent, and landing)

are given in Table 3. Additionally, the performance requirements for the aircraft are given in Table 2. A summary of the equations used to calculate the power demand of the VTOL-type aircraft is given in Table 4. For the meaning of the symbols in the equations please refer to the nomenclature at the end of the paper.

Table 2. Mission requirements for the aircraft flight modes (adapted from the Uber report [7]).

Flight Mode	Vertical Speed (m/s)	Horizontal Speed (m/s)	Altitude (m)
Hover *(1)*	0 to 2.54	0	15.24
Transition+climb *(2)*	2.54	0 to 1.2 V_{stall}	91.44
Accel+climb *(3)*	2.54	1.2 V_{stall} to 67	457.2
Cruise *(4)*	0	67	457.2
Decel+descend *(5)*	2.54	67 to 1.2 V_{stall}	91.44
Transition+descend *(6)*	2.54 to 1.52	1.2 V_{stall} to 0	15.24
Hover descend *(7)*	1.52 to 0	0	0

Table 3. The performance requirements for modes of the aircraft.

Constraints	Value
Battery power density	2800 W/kg [10]
Fuel cell power density	1500 W/kg [20]
Cruise speed	150 mph (67 m/s)
Range	60 mile (96 km)
Maximum dimension of length and height	50 ft - 20 ft (15.2 m - 6.1 m)
Ground taxi speed	5 ft/sec (1.524 m/s)
Payload mass	445 kg (a pilot and 3 or 4 passengers including luggage)
Maximum battery charging time	7 minutes

Table 4. Equations for power demand estimates of the aircraft flight modes [21]-[23].

	Flight Mode	Propulsive ower demand estimation equations	Flight time	Fuel cell or battery	eq.
1	Hover	$\sum_{j=1}^{NR} T_j \left[k_i \sqrt{\frac{DL}{2\rho}} + \frac{\rho V_{tip}^3}{DL} \left(\frac{\sigma C_{d0}}{8} \right) \right]$	t_1	Battery	(1)
2	Transition+climb	$\sum_{j=1}^{NR} T_j \left[V_y - \frac{k_i}{2} V_y + \frac{k_i}{2} \sqrt{V_y^2 + \frac{2DL}{\rho}} + \frac{\rho V_{tip}^3}{DL} \left(\frac{\sigma C_{d0}}{8} \right) \right]$	t_2	Battery	(2)
3	Accel+climb	$\frac{W}{\eta} \left(RC + \frac{1}{\frac{C_L}{C_D}} \sqrt{\frac{2}{\rho} \frac{1}{\sqrt{C_{Dmin}\, \pi\, AR\, e}}} \sqrt{\frac{W}{S}} \right)$	t_3	Fuel cell	(3)
4	Cruise	$W \sqrt{\frac{2}{\rho} \left(\frac{W}{S} \right)} \frac{4 C_{D,0}}{(3\, C_{D,0}\, \pi\, e\, AR)^{0.75}}$	t_4	Fuel cell	(4)
5	Decel+descent (5)	Assumed equal to power demand in accel+climb flight mode.	t_5	Fuel cell	
6,7	Landing (6, 7)	No power demand calculation has been made. It is assumed that the aircraft is approximately equal to the take-off power.	t_{6-7}	Battery	

There is great variation in power demands in all flight modes of an aircraft and the power demand of take-off flight mode is greater than in other flight modes. Accordingly, it is planned to meet the power demand of the VTOL according to the battery or the fuel cell as reported in Table 4. In particular, battery is used for the higher power phases while the fuel cell is used in the central part of the flight. In the present investigation, the possibility of using both systems is not considered.

2.2. Weight analysis of the lift-cruise aircraft

The propulsion system of the aircraft generally consists of the Li-ion battery, a propeller, a PEM fuel cell, an electric motor, the electronics that implement the sum of the electricity (energy management system EMS), and a pressurized hydrogen storage system (Figure 3).

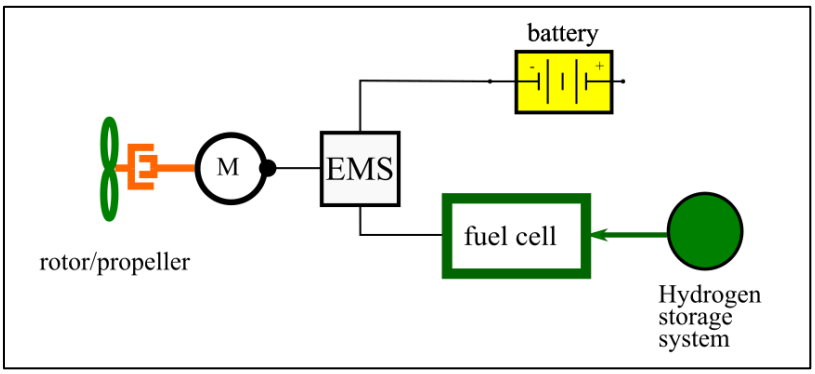

Figure 3. Scheme of the propulsive system.

The total weight of the aircraft is expressed by eq. (5).

$$W_{total} = W_b + W_{fc} + W_{hss} + W_{EM} + W_{av} + W_{af} + W_{pl} \quad (5)$$

where W_b, W_{fc}, W_{hss}, W_{EM}, W_{EMS}, W_{av}, W_{af}, W_{pl} are the weight of battery, fuel cell, hydrogen storage, electric motor, energy management system, avionics, airframe, payload, respectively.

The size of battery and fuel cell in the hybrid propulsion system are determined from the sizing optimization problem described in the next sections. Then, their weight is calculated by assuming for the battery (PD_{bat}) and fuel cell (PD_{FC}) power densities 2800 and 1500 W/kg respectively [10][20][24] and 200Wh/kg was assumed for the energy density of the battery. It should be noted here that a complete discharge of the battery damages the life of the battery and, therefore, the battery was sized by assuming that only 70 percent of its nominal energy can be used in the flight.

The following equations details the calculation of W_b, W_{fc} and W_{hss}.

$$W_{fc} = g\frac{P_{fc}}{PD_{fc}} \quad (6)$$

$$W_b = g\frac{Ebatt}{ED_{bat}} \quad (7)$$

where P_{fc}, PD_{fc}, $Ebatt$ and ED_{bat} are the fuel cell power, the fuel cell power density, the battery energy and the battery energy density, respectively.

The mass flow rate of hydrogen consumed by the fuel cell in the propulsion system is calculated by [25]:

$$H_{2,flow\,rate} = 1.05 * 10^{-8} FC_{power}/0.65 \quad (8)$$

Where 0.65 is the cell voltage in Volt which is assumed constant for this preliminary analysis as suggested in [25]. Actually, the cell voltage is a measure of the efficiency of the fuel cell and, depending on the current load, ranges usually between 0.6 V and 0.7 V in a PEM fuel cell.

Since the fuel cell provides power in cruise, accel+climb, decel+descend flight modes, the hydrogen mass can be calculated by multiplying the mass flow rate with the flight time. The hydrogen masses calculated for each flight mode are added together to calculate the total required hydrogen mass $m_{hydrogen}$.

For the storage unit, an efficiency of 5 percent is assumed, i.e. the store mass of hydrogen is 5% of the total mass of the hydrogen storage system [26]. Therefore:

$$W_{hss} = g\frac{m_{hydrogen}}{0.05} \tag{9}$$

The electric machine and the propeller are sized according to the maximum power request in the flight. The power-to-weight ratio of the motor (inclusive of its controller) is assumed equal to 5 kW/kg [20]. The motor and propeller efficiencies are assumed equal to 0.95 and 0.82, respectively [24]. For the weight of energy management system, avionics, airframe, and payload, the assumed masses are 50, 200, 900, and 445 kg, respectively [6][7].

2.3. Formalization of the optimization problem

The sizing optimization proposed in this study is carried out according to the minimum power consumption of the aircraft the central part of the mission, i.e., the power of the fuel cell. Therefore, the maximum of the power demand in phases 3, 4 and, 5 is the objective function in the optimization problem [27][22].

$$J = P_{FC} = PD_{FC} \cdot M_{FC} = \max(P_3, P_4, P_5)/\eta_{EM,P} \tag{10}$$

Where, PD_{FC}, and M_{FC} represent power density of fuel cell (W/kg), and fuel cell mass (kg), respectively. The $P_3 - P_5$ represents the power demands of the aircraft according to the flight modes powered by the fuel cell (Table 4) and $\eta_{EM,P}$ is the product of the efficiencies of the propeller and the electric machine. In other words, $\eta_{EM,P}$ is the ratio between the electric power demand to be fulfilled by the battery or the fuel cell and the propulsive power (calculated as in Table 4), taking into account all losses in the propeller-motor system.

The battery is sized according to the following reasoning. Since the battery is responsible for the hover, transition+climb, and landing flight modes, it must have more power than is demanded in these flight modes.

$$P_{batt} = PD_{batt} \cdot M_{batt} \geq \max(P_1, P_2, P_{6,7})/\eta_{EM,P} \tag{11}$$

However, it is also necessary to verify that the battery is able to satisfy the energy request:

$$E_{batt} = ED_{batt} \cdot M_{batt} \geq \frac{(P_1 \cdot t_1 + P_2 \cdot t_2 + P_{6-7} \cdot t_{6-7})/\eta_{EM,P}}{DOD} \tag{12}$$

In the equations above, PD_{batt} and M_{batt} represent power density of battery (W/kg) and battery mass (kg),) respectively. The terms $P_1, P_2 P_{6,7}$ represent the power demand of the aircraft according to the flight modes powered by the battery in Table 4. In order not to shorten the life of the batteries, a Depth of Discharge (DOD) of 70 percent is considered as explained before.

Equations (13)-(16) express the constraints of the optimization problem of the aircraft architecture. In particular, eq. (13) states the relationship of cruise speed with wind load, aspect ratio, and zero-lift drag ratio. The constraint related to wing loading is represented by eq (14). The third equality constraint concerns the aspect ratio and specifies its relationship to wing loading, zero lift-drag ratio, and cruise speed, eq. (15). Finally, the difference between stall and cruise velocities is the inequality constraint (16) in the sizing problem.

$$V_{cr} = \left(\frac{2}{\rho} \left(\frac{W}{S} \right) \sqrt{\frac{1}{3C_{D,0}\, \pi\, e\, AR}} \right)^{1/2} \tag{13}$$

$$\frac{W}{S} = \frac{\rho V_{stall}^2 C_{L,max}}{2} \tag{14}$$

$$\sqrt{AR} = \left[\frac{2}{\rho} \left(\frac{W}{S} \right) \sqrt{\frac{1}{3\, C_{D,0}\, \pi\, e}} \right] \frac{1}{V_{cr}^2} \tag{15}$$

$$S_{dmin} \geq V_{cr} - V_{stall} \tag{16}$$

In these equations, V_{cr}, $\frac{W}{S}$, e, AR, $C_{D,0}$, S_{dmin}, and V_{stall} represent cruising velocity (m/s), wing loading (N/m2), Oswald efficiency factor, aspect ratio, Zero-lift drag coefficient, minimum velocity difference, and stall velocity, respectively.
The optimal values of the design variables are determined by solving the following optimization problem:

$$\begin{array}{ll} minimize & f(P_{FC}) \\ with\ respect\ to & x = (WL, AR, \mathrm{C_{lmax}}, \mathrm{V_{stall}}, \mathrm{V_{cr}}, \mathrm{P_{bat}}, \mathrm{C_{D,0}}, DL, \sigma) \\ subject\ to & \text{bounds of variables and constraints (11)-(16)} \end{array}$$

This problem has been solved with the "interior-point" algorithm which is included in MATLAB optimization routine and is used to solve multivariate nonlinear problems [28][18].

The limits of the design variables and the optimal value found with the application of the optimization algorithms are shown in Table 5.

Table 5. Bounds for the design variables and results of the optimization.

Variable	WL	AR	C_{lmax}	V_{stall}	V_{endure}	Battery Power	$\mathbf{C_{D,0}}$,	DL	$\boldsymbol{\sigma}$	J
Unit	N/m^2			m/s	m/s	kW		N/m^2		kW
Lower bound	90	8	1	5	5	10	0.025	10	0.1	
Upper bound	200	20	1.25	20	20	200	0.045	20	0.2	
Optimal value	200	8	1.16	16.7	20	57	0.025	10.37	0.11	43.07

3. Results and discussion

The mass ratios of the optimized aircraft with a total mass of 1800 kg are reported in Figure 4 while the power demand of each phase of flight is reported in Figure 5 together with the details of the propulsion system that accounts for about 10% of the take-off weight. The power demand for the hover, transition+climb, accel+climb, and cruising flight modes of the aircraft are calculated as 54.2, 48.1, 43, and 15.3 kW, respectively. This has led to the choice of a fuel cell of 43 kW while the power required from the battery is 54.2 kW keeping into account the efficiency of the motor and the propeller (Figure 5).

The energy required by the different flight modes and the available energy of the battery and hydrogen are given in Figure 6 for comparison. Again, the efficiency of all up-stream devices was taken into account in the sizing of the battery and the stored hydrogen. In addition, the hydrogen flow rates calculated are given in Table 6. Accordingly, it has been observed that there is more hydrogen consumption in accel+climb flight mode than in cruising flight mode. The total hydrogen consumption

is about 0.65 kg while the mass of the hydrogen storage system is calculated as approximately 13 kg according to eq. (9).

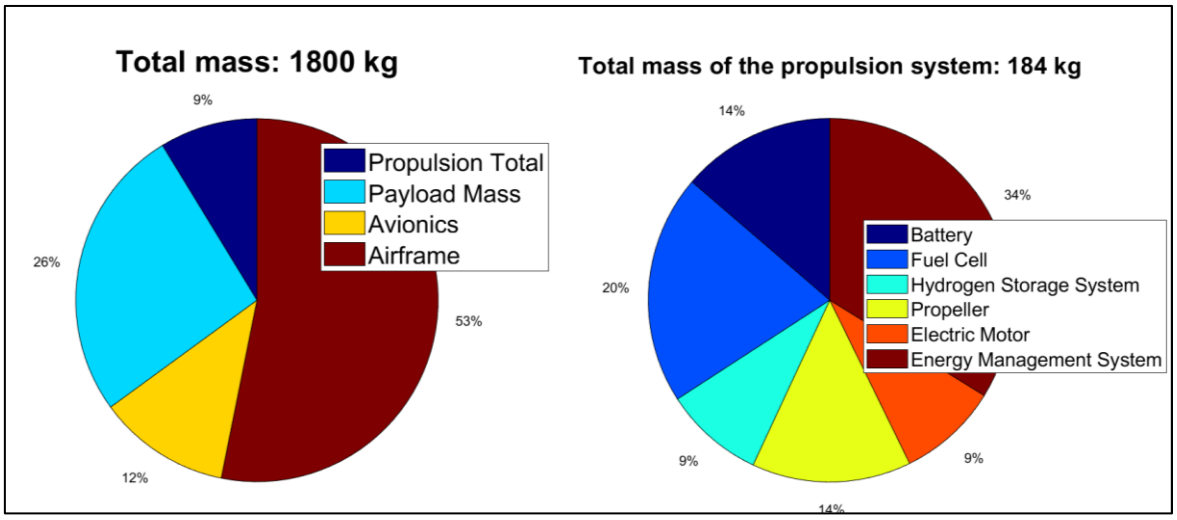

Figure 4. Final mass ratios of the eVTOL aircraft.

The overall consumption of energy of the mission is, therefore, 0.65 kg of H2 and 3.3 kWh of electricity.

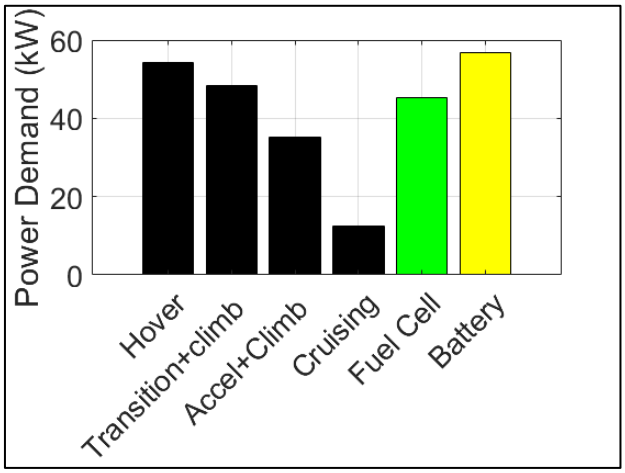

Figure 5. The power demands according to flight modes of the eVTOL aircraft together with the final size of the fuel cell.

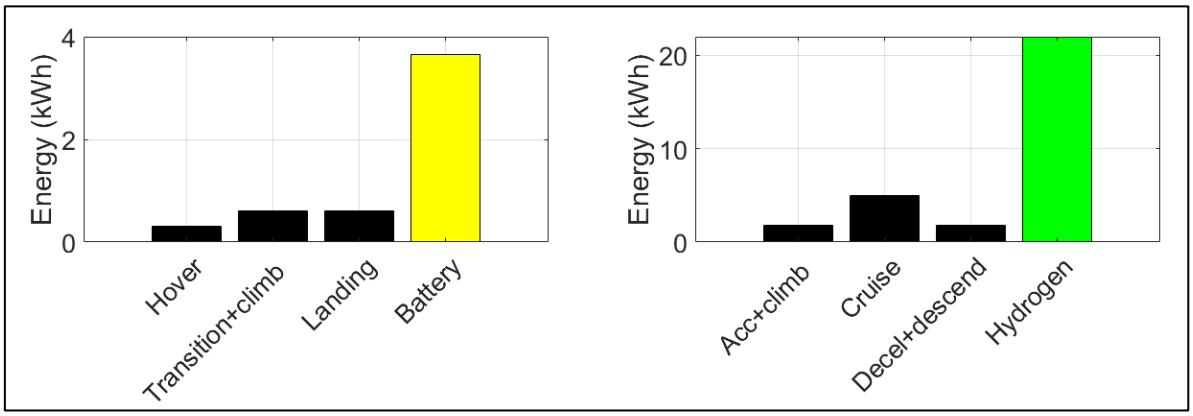

Figure 6. Energy demand and availability.

Table 6. Hydrogen flow rate according to flight modes.

Hydrogen flow rate	
Hydrogen flow rate for accel+climb	0.73 g/s
Hydrogen flow rate for cruising	0.26 g/s

3.1. Consideration on the environmental impact

Electric aerial vehicle powered by battery and/or fuel cells are often considered as zero emission transportation systems. This is true from a local point of view since no greenhouse and pollutant emissions are generated during the flight. However, electricity and hydrogen are energy carriers that can be produced by a variety of energy sources and conversion processes.

According to the European Energy Agency (EEA [18]), the greenhouse Emission Intensity or electricity production in EU in 2019 is, on average, 275.0 g CO2/kWh with a maximum of 891 g CO2/kWh for Estonia and a minimum of 8 g CO2/kWh for Sweden as shown in Figure 3a, where the value for Italy is also shown. However, the greenhouse emission intensity is expected to be reduced significantly in the next future.

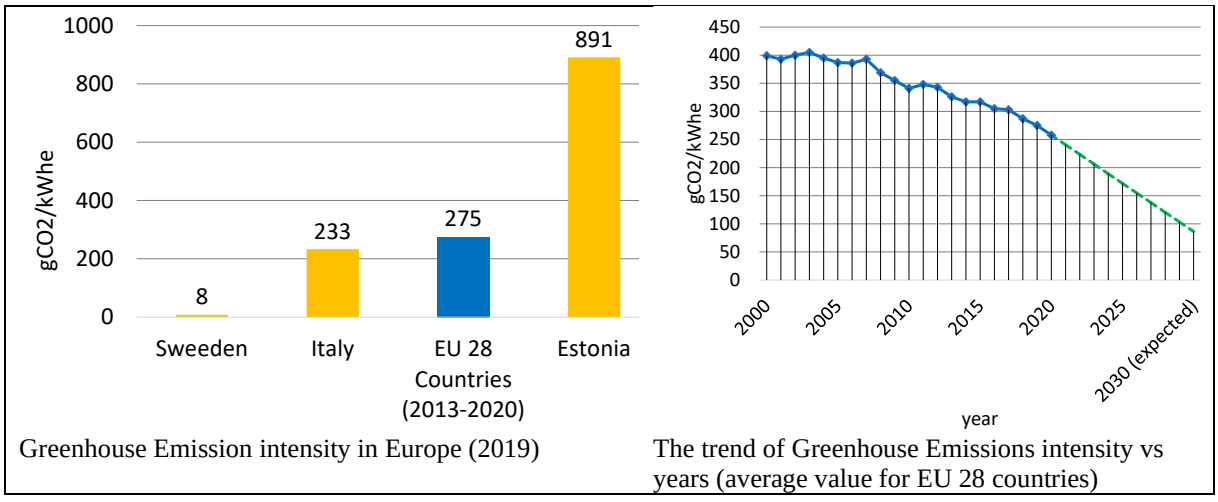

Greenhouse Emission intensity in Europe (2019)

The trend of Greenhouse Emissions intensity vs years (average value for EU 28 countries)

Figure 7. Past, today's and future Emission Intensity of European countries (www.eea.europa.eu).

As for the hydrogen, the main production methods and the corresponding CO2 emission intensity (HEI) are shown in

Table **7** [19] even if this topic is quite vast and many other production systems can be employed for the production of hydrogen, like for example biomass gasification [29].

Table 7. Main production methods for hydrogen production and the corresponding emission intensity.

Method	Energy Source	Hydrogen Emission Intensity in kg_{CO2}/kg_{H2}
Black Hydrogen	Coal	20
Grey Hydrogen	Natural gas	8.5
Blue Hydrogen	Coal with Carbon Capture, Utilization, and Storage (CCUS)	2.4
	Natural gas with CCUS	1
Green Hydrogen	Renewable electricity	0

The emissions associated to the electricity consumption can be estimated as:

$$CO_2, elec = EI \cdot \frac{E_{tot}}{\eta_{charge} D} \quad (17)$$

Where EI is the Emission Intensity, E_{tot} is the total electricity consumed in the emission (in kWh), D is the total travelled distance (108km in this investigation) and η_{charge} is used to take into account the losses in the electric grid and in the charging process (0.8).

The emissions associated to the use of hydrogen are calculated as:

$$CO_2, H_2 = HEI \cdot \frac{m_{hydrogen}}{D} \quad (18)$$

Where HEI is the Hydrogen Emission Intensity and $m_{hydrogen}$ is the total among of hydrogen consumed in the emission (in kg).

The equations (17) and (18) were used to obtain the plot of Figure 8 where a full electric aerial vehicle with the same mass is reported for comparison. For this vehicle, an electric consumption of 0.53 kW/km was obtained in [9]. It can be noticed that, except for the case of black hydrogen, the emissions are below 80g/km even with very high values of electricity emission intensity. In the case of blue hydrogen, the emissions are lower than that of the full electric vehicle except that for very low values of EI. Of course, in the case of electricity from renewable energy sources both aerial vehicles (full electric and hydrogen hybrid electric) can be considered "zero emission" from a Well-to-Wing point of view.

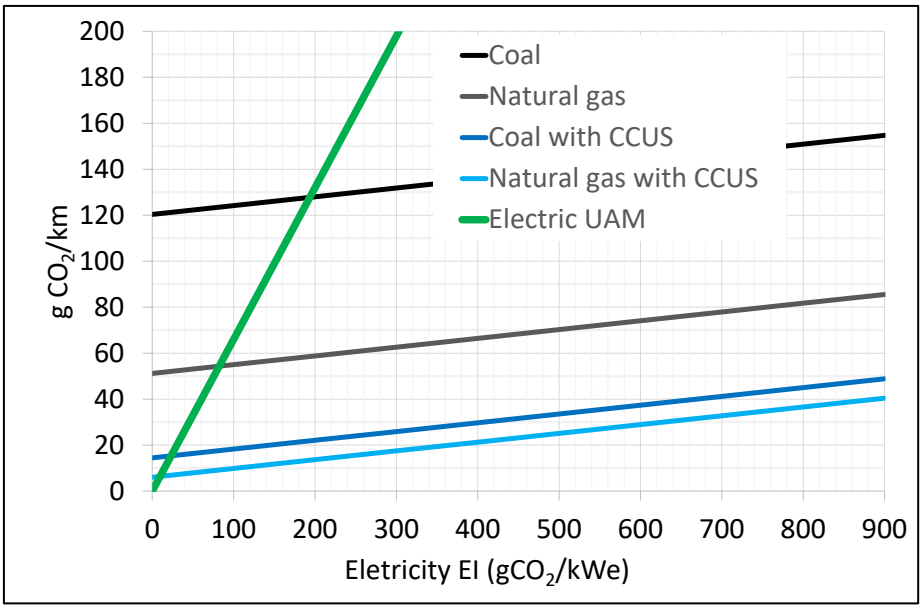

Figure 8. Indirect environmental impact.

4. Conclusions

In this study, the optimal sizing of the hybrid propulsion system of a lift-cruise eVTOL for passenger transportation in urban air mobility is carried out. This hybrid propulsion system consists of a PEM-type fuel cell and a Li-ion-type battery. The power demand of the aircraft at each flight stage is calculated with the general flight dynamics equations, and an optimization problem is performed that minimizes the power demand by keeping constant the flight time. In this optimization study, battery power, wing loading, cruising speed, aspect ratio, and the difference between stall speed and cruising velocity are defined as design variables of the problem. In addition, battery and fuel cell weights are obtained from the optimization problem and a weight analysis study is carried out for the aircraft. It is foreseen that the study will be beneficial for aircraft designers and to compare different types of VTOL aircraft configurations for urban air mobility also in terms of indirect environmental impact.

5. Nomenclature

Abbreviation

AFC	Available fuel cell power
B	Battery
D	Travel distance
DOD	Depth of Discharge
EM	Electric motor
ED	Energy density
EI	Emission Intensity
EMS	Energy management system
HEI	Hydrogen emission intensity
LHV	Lower heating value of hydrogen
NR	Number of rotors
PD	Power density
PEM	Proton membrane exchange
UAV	Unmanned aerial vehicle
UAM	Urban air mobility
eVTOL	Electric vertical take-off and landing

Subscripts

av	Avionic
af	Airframe
b, bat	Battery
cr	Cruise
cl	Climb
en	Endurance
em	Electric machine
fc	Fuel cell
hss	Hydrogen storage
h	Hydrogen
p	Propeller
pl	Payload
tot	Total

Mathematical Symbols

AR	Wing aspect ratio
$C_{D,min}$	Minimum drag coefficient
$C_{L,max}$	Maximum lift coefficient
$C_{D,0}$	Zero-lift drag coefficient
DL	Disk loading
e	Oswald efficiency factor
E	Energy
g	Gravitational acceleration
k_i	Induced power factor
M	Motor
m	Mass
P	Power
RC	Rate of climb
S	Wing Area
S_{dmin}	Minimum velocity difference
t	Flight time
T	Thrust
V	Velocity
V_{cr}	Crusing velocity
V_{tip}	Rotor's blade tip velocity
V_y	Vertical velocity
V_{stall}	Stall velocity
W/S	Wing loading
W	Weight

Greek symbols

ρ	Density
η	Efficiency
σ	Rotor's Solidity

References

[1] Garrow L A, German B J, and Leonard C E 2021, *Transp. Res. Part C Emerg. Technol*., **132**, 103377 doi: 10.1016/j.trc.2021.103377.
[2] Cohen A, Shaheen S 2021, *Int. Encycl. Transp.*, pp. 702–709, doi: 10.1016/b978-0-08-102671-7.10764-x.
[3] Palaia G, Salem K A, Cipolla V, Binante V, Zanetti D 2021, *Appl. Sci*., **11**, 22, doi: 10.3390/app112210815.
[4] Rothfeld R, Straubinger A, Fu M, Al Haddad C, Antoniou C 2019, *Demand for Emerging Transportation Systems, Urban air mobility*, ed Antonious C, Efthymiou D, Chaniotakis E (Amsterdam: Elsevier) Chapter 13, doi: 10.1016/B978-0-12-815018-4.00013-9.
[5] Kadhiresan R, Duffy M J 2019, *AIAA Aviat. 2019 Forum,* pp. 1–19,doi: 10.2514/6.2019-2873.
[6] Ahluwalia R K, Peng J K, Wang X, Papadias D, Kopasz J 2021 *Int. J. Hydrogen Energy*, **46**, 74, pp. 36917–36929, doi: 10.1016/j.ijhydene.2021.08.211.
[7] https://s3.amazonaws.com/uber-static/elevate/Summary+Mission+and+Requirements.pdf, retrieved online on 10 July 2022

[8] Polaczyk N, Trombino E, Wei P, Mitici M 2019 *8th Biennial Autonomous VTOL Technical Meeting and 6th Annual Electric VTOL Symposium*, (Vertical Flight Society) pp. 333–343
[9] Donateo T, Ficarella A 2022, *Energies*, **22**,15, 638. https://doi.org/10.3390/en15020638.
[10] Nadir M, Zhou Z, Benbouzid M 2019 *Applied Energy*, **255**, https://doi.org/10.1016/j.apenergy.2019.113823
[11] Ouyang L, Huang J, Wang H, Liu J, Zhu M 2017, *Mater. Chem. Phys.*, **200**, pp. 164–178, 2017, doi: 10.1016/j.matchemphys.2017.07.002.
[12] Hall P J, Bain E J 2008, *Energy Policy*, **36**, 12, pp. 4352–4355, doi: 10.1016/j.enpol.2008.09.037.
[13] Wang B, Zhao D, Li W, Wang Z, Huang Y, You Y, Becker S 2020, *Prog. Aerosp. Sci.*, **116**, no. May, p. 100620, 2020, doi: 10.1016/j.paerosci.2020.100620.
[14] Chang X, Kong B, Gholizadeh F 2022, *Energy Sources, Part A: Recovery, Utilization and Environmental Effects*, **44**, 2 https://doi.org/10.1080/15567036.2022.2061645
[15] Oh T H 2018, *Energy Convers. Manag.*, **176**, no. July, pp. 349–356, doi: 10.1016/j.enconman.2018.09.036.
[16] An J H, Kwon D Y, Jeon K S, Tyan M, and Lee J-W 2022, *Aerospace*, **9**, 2, pp. 1–26, doi: 10.3390/aerospace9020071.
[17] Boukoberine M N, Donateo T, Benbouzid M 2022, *IEEE Transactions on Energy Conversion*, **37**, 3, doi: 10.1109/TEC.2022.3152351.
[18] Ang BW, Su B 2016, *Energy Policy*, **94**, pp 56-63, doi: 10.1016/j.enpol.2016.03.038.
[19] Yu M, Wang K, Vredenburg H 2021, *International Journal of Hydrogen Energy*, **46**, 41, doi: 10.1016/j.ijhydene.2021.04.016
[20] Afonso F, Ferreira A, Ribeiro I, Lau F, Suleman A, 2021, *Transp. Res. Part D Transp. Environ.*, **91**, January, 2021, doi: 10.1016/j.trd.2020.102688.
[21] Seddon J, Newman S 2011, *Basic Helicopter Aerodynamics*, (New York: Wiley)
[22] Anderson J D 1989, *Introduction to Flight*, 3rd Edition (New York: McGraw-Hill)
[23] Anderson J D 1999 *Aircraft performance and design*, (New York: McGraw-Hill)
[24] Cakin U, Kacan Z, Aydogan Z A, Kuvvetli I 2020, *Aiaa Aviat. 2020 Forum*, **1,** PartF, pp. 1–17, doi: 10.2514/6.2020-3173.
[25] Larminie J, Dicks A 2013, *Fuel cell systems explained:* Second edition (Chichester: Wiley)
[26] https://www.energy.gov/eere/fuelcells/physical-hydrogen-storage, accessed on 1 March 2022.
[27] Raymer, D P 2018, *Aircraft Design: A Conceptual Approach*, Sixth Edition (Reston, VA: AIAA)
[28] Harmon F G, Frank A A, Chattot J J 2006, *J. Aircr.*, **43**, 5, pp. 1490–1498, doi: 10.2514/1.15816.
[29] Koroneos C, Dompros A, Roumbas G 2008, *Chemical Engineering and Processing: Process Intensification*, **47**, 8, doi: 10.1016/j.cep.2007.04.003